KFUPM
Journal of Undergraduate Research International

Diamond Open Access 189

Article Petroleum Engineering

Sensitivity Analysis of Dynamic Wettability Alteration Effects on CO_2 Saturation Front in Aquifers

Khaled Muteb Alrashidi and Arshad Raza*

Cite https://doi.org/10.64589/juri/231595

Submitted: April 28, 2026 **Revised:** May 18, 2026 **Accepted:** May 21, 2026

ABSTRACT

As Carbon Capture and Storage becomes key for mitigating climate change, the time-dependent behavior and interactions between CO_2, native rock, and subsurface fluids must be understood. Recent studies have revealed the effect of wettability alteration (WA) on plume migration and trapping, yet the associated pressure behavior within reservoirs has not been given attention. This study investigates the effects of dynamic WA during constant-rate CO_2 injection into saline aquifers. Numerical experiments were conducted to determine the potential deviations caused by time-dependent alteration in the CO_2 saturation front extent. A one-dimensional model was used, which assumes two end states of wettability: a water-wet case (Case A) and an intermediate-wet case (Case B), with a dynamic morph between the two end states controlled by a mixing parameter. The alteration model was coupled sequentially using a MATLAB reservoir simulation toolbox simulation, in which the exposure time and wettability factor were updated externally after the macro-steps. The results showed that the saturation front was sensitive to parameters controlling the alteration, particularly the onset saturation threshold. Lower onset saturation values enabled alterations to accumulate in a larger part of the plume and could significantly change the front location, whereas the maximum alteration parameter showed a limited response under the evaluated conditions. The simplified model reveals that wettability alteration suppresses front migration and enhances front sharpness, providing insight into how wettability effects influence displacement dynamics.

Keywords: CO_2 storage, saline aquifers, dynamic wettability alteration, MRST, relative permeability, saturation front

1. INTRODUCTION

Climate change is a pressing global challenge primarily driven by anthropogenic CO_2 emissions released through industrial processes, energy production, and land-use changes [10]. The continuous accumulation of greenhouse gases in the atmosphere has increased global warming, leading to rising temperatures, melting ice caps, and severe environmental impacts that threaten ecosystems and human livelihoods. The urgent need to mitigate these emissions has spurred worldwide efforts toward decarbonization and the adoption of sustainable technologies. Carbon Capture and Storage (CCS) has been widely recognized as one of the most promising approaches to achieving significant emission reductions, particularly in hard-to-abate industries such as cement, steel, and chemicals [11]. These industries are fundamental to modern economies but remain heavily dependent on fossil fuels, making direct substitution with renewable energy sources challenging in the short term.

The CCS process captures CO_2 directly from large point sources, such as power plants and industrial facilities [1], transporting it through pipelines or ships, and securely storing it in suitable geological formations, with short- and long-term monitoring to prevent its release into the atmosphere. This process enables the continued use of existing energy and industrial systems while significantly reducing their carbon footprint. Among the various explored storage options, such as depleted oil and gas reservoirs, unmineable coal seams, and deep saline aquifers, the latter has the greatest potential for large-scale, long-term CO_2 sequestration [9].

However, the successful deployment of CCS relies on a comprehensive understanding of the physical and chemical interactions that occur within these reservoirs during and after CO_2 injection. Factors such as reservoir heterogeneity, pressure management, CO_2 plume migration, and mineralization reactions must be thoroughly investigated to ensure long-term stability and safety. Therefore, the advancement of research on storage mechanisms, monitoring techniques, and modeling tools is critical for enhancing the reliability and cost-effectiveness of CCS systems. As global efforts intensify to achieve net-zero emission targets by the mid-century, CCS in deep saline aquifers has become a cornerstone technology for bridging the gap between current fossil-based systems and a sustainable, low-carbon future.

As CCS garners attention as a key mechanism for mitigating climate change, it needs to be scaled up, which requires a thorough understanding of the time-dependent behavior and interactions between CO_2, native rock, and subsurface fluids. This clarification will enable accurate risk assessment and facilitate the design of optimal injection and storage programs. Motivated, this study focuses on investigating the effects of CO-induced

Published under an exclusive license by KFUPM

wettability alteration (WA) and the resulting changes in saturation functions on injection safety. A lack of understanding of the dynamic effects of WA could lead to inaccurate modeling of injection behavior and storage performance.

This study mainly aims to investigate the effects of dynamic WA during constant-rate CO_2 injection in saline aquifers, as it affects the relative permeability. Through numerical experiments using a one-dimensional (1D) model, it reveals the potential deviations caused by dynamic alterations in the saturation front. It extends WA modeling to describe WAs and the effects of the model parameters on the CO_2 plume. An understanding of these dynamics is pivotal for well placement, risk assessment, and history matching, as it will indicate the potential trends and behaviors associated with variations in the wetting state of the rocks owing to prolonged exposure to CO_2.

1.1. Background on WA. This section presents an overview of recent work on the role of wettability in field-scale behavior and the experimental studies that showcase dynamic shifts. This section also provides modeling approaches used to incorporate these shifts and the reported field-scale implications of the dynamic shifts.

Wettability is a property that describes multiphase flow in porous media. This parameter governs the distribution of fluids inside a pore system and controls the flow parameters in multiphase flow, mainly the capillary pressure and relative permeability. The relative permeability of the wetting phases is lower than that of the non-wetting phases because the wetting phases tend to stick to the surface of the rock[4].

Simulation studies have investigated the effects of static wettability conditions on CO_2 storage, noting that the parameters used in these models are typically static representations of the rock wetting state. For example,[2] conducted a simulation study to investigate the effects of five different wetting states ranging from strongly water-wet to strongly CO_2-wet. They found that CO_2-wet reservoirs are generally unfavorable for containment, as they enable the highest CO_2 vertical migration and reduce the residual trapping capacity. They also observed that CO_2-wet conditions induce an increased areal extent of the plume, which in turn, increases solubility trapping owing to the expansion of the contact interface area.[12] simulated the impact of strongly water-wet versus strongly CO_2-wet sandstone systems, neglecting the effects of dynamic capillary pressure. They found that the water-wet sandstone system exhibited a 42% higher residual trapping than the CO_2-wet system. By contrast, the CO_2-wet scenario exhibited significantly higher plume migration heights during storage and yielded larger solubility trapping, with approximately 20% more dissolved CO_2 observed in CO_2-wet sandstones.

Experimental studies have shown that wettability is not static, and CO_2 exposure alters it from the original water-wet condition toward CO_2-wet conditions.[3] conducted an aging experiment and confirmed that wettability evolves significantly over time in CO_2-brine–rock systems. After two weeks of CO_2-brine exposure at 50 °C and 10 MPa, both the Berea sandstone and Indiana limestone experienced an increase in contact angle; the sandstone transformed from a strongly water-wet to weakly water-wet condition, and the contact angle increased from 15.6°to 67.7°. By contrast, the limestone sample transitioned from initial complete absorption of the droplet to an angle of 79.7°.

This alteration is accompanied by characteristic variations in the capillary pressure and relative permeability based on the underlying mineralogy and reaction kinetics. For example,[6] examined Berea sandstone samples and observed that wetting conditions significantly changed from strongly water-wet to mixed-wet systems, which was attributed to clay dissolution or a decreased hydrophilicity of quartz. Reactive flow resulted in CO_2 exposure, reducing the capillary entry pressure by 20 psi to almost 50 psi, and relative permeability measurements confirmed that the samples became more CO_2-wet after exposure. However, their finding that the overall permeability increased owing to dissolution contradicts another sandstone study by[5], who found that despite clay dissolution, both CO_2 relative permeability and absolute permeability decreased from 185±10 to 110±8 mD. These declines were attributed to the migration of fine particles, specifically the accumulation of kaolinite that blocked small pores and throats, impeding flow with the increase in the total porosity. A CO_2-induced transition toward weakly water-wet conditions and a corresponding reduction in calculated capillary pressure were observed.

Dynamic shifts owing to reactive transport have not been included in standard simulation studies. Two key areas of work appear when considering modeling of dynamic WAs: the studies by Kassa et al. (2020, 2021) and Zhang et al. (2025). Kassa et al. (2020) applied a direct interpolation between two end states of the capillary pressure curve using a morph weight omega, where omega is a Langmuir-type function of exposure time χ and a calibration parameter β that governs the steepness and is related to the pore-scale parameter C obtained from the bundle-of-tube simulation. Kassa et al. (2021) considered two approaches for relative permeability shifting: either a morph of the relative permeability curves, as implemented in the capillary pressure modeling in Kassa et al. (2020), or a morph of the parameters that parameterize the relative permeability curves. They used a reduced LET model and found that the morph of the parameters was more accurate and yielded consistent results.

Zhang et al. (2025) proposed a simplified framework for practicality. The framework introduces a single, linear transition function governed only by the cumulative CO_2 exposure time, t_e, and a global transition duration, T. This function uniformly maps all wettability-dependent properties, including the capillary entry pressure, relative permeability, and residual trapping coefficient, from their initial strongly water-wet to final weakly water-wet states. Unlike Kassa's formulation, which uses a nonlinear Langmuir shape and pore-scale calibration constant β, this model assumes linear evolution and regards T as a phenomenological timescale that encapsulates the overall rate of alteration.

Kassa et al. (2022) and Zhang et al. (2025) investigated the field-scale consequences of this time-dependent transition from water-wet conditions. Both studies found that WA significantly influenced the plume behavior and trapping efficiency. Regarding plume migration, both studies demonstrated that dynamic alteration influences flow dynamics in the reservoir. WA caused the plume migration fronts to sharpen and delay in horizontal flow systems compared to static water-wet systems. WA also resulted in more extensive plume extent, causing the plume in the final, less water-wet state to migrate upward and its height to steadily increase with storage time. Their findings are consistent

Table 1. *Summary of experimental studies on WA owing to CO_2*

Study	Rock Type	Wettability Trend	Capillary Pressure Trend	Relative Permeability Trend	Key Findings
Alsalman et al. (2024)	Berea sandstone and Indiana limestone	Wettability evolves significantly over time; sandstone shows a change in contact angle from 15.6°to 67.7°; limestone transforms from complete droplet absorption to a contact angle of 79.7°	-	-	Two weeks of CO_2-brine exposure at 50 °C and 10 MPa causes substantial WA in both sandstone and limestone.
Gholami and Raza (2022)	Berea sandstone	Strongly water-wet to mixed-wet condition	Decrease in capillary entry pressure (-20 to -50 psi)	Increase in Kr (more CO_2-wet behavior)	CO_2 exposure and clay dissolution reduced hydrophilicity of quartz; the overall permeability increased.
Chai et al. (2025)	Sandstone	Slight shift toward weakly water-wet	Reduced Pc	Decline in CO_2 Kr and absolute permeability (185 to 110 mD)	Fines migration blocked the pores, despite dissolution; reduced flow capacity.
Fatah et al. (2021)	Shales (Eagle Ford, Wolfcamp, Mancos)	Clay-rich: transforms from water-wet to CO_2-wet; quartz-rich: remained water-wet	-	-	Mineralogy controls wettability: clay promotes CO_2-wet shift; quartz preserves hydrophilicity.
Farokhpoor et al. (2013)	Individual minerals	Quartz/feldspar/calcite unchanged; muscovite changed from water-wet to less water-wet	-	-	Long-term CO_2 exposure reduces wettability of mica, potentially decreasing caprock sealing efficiency.
Wang and Tokunaga (2015)	Limestone/ dolomite sands	Water-wet to mixed-wet	Lower Pc for brine than predicted by upscaling	-	Shifts in Pc curves after exposure indicate potential WA.
Kim et al. (2012)	Silica micromodels	Strongly water-wet to less water-wet (contact angle increases from 0°to 80°)	-	-	Increased salinity amplifies CO_2-induced dewetting; pore-scale evidence of WA.

with those of studies on static wettability conditions, suggesting a potential for capillary leakage.

In addition, WA was found to be detrimental to residual trapping. Zhang et al. (2025) showed that if WA progresses fully, the residual trapping capacity decreases by 49.7% compared to the initial strongly water-wet state, primarily because of the release of previously trapped CO_2. However, the larger areal extent of the plume caused by WA enhanced dissolution trapping, resulting in a 5.2% increase in dissolution trapping in the long-term WA case compared with the static strongly water-wet case.

Although recent studies have revealed the effect of WA on plume migration and trapping, the associated pressure behavior within reservoirs has not been investigated in detail. A gap also exists in our understanding of aquifer behavior under spatially varying dynamic WA potentials. To address this gap, this study investigates and quantifies the influence of WA on reservoir pressure evolution by adopting a similar modeling strategy to that reported by Zhang et al. (2025).

2. METHODOLOGY

2.1. WA Modeling. Two end states of wettability were assumed in the modeling: a water-wet case (Case A) and a weakly water-wet case (Case B). The dynamic morph between the two end states provided a saturation function for a given grid block. The modeling focused on the relative permeability, *K*r. This approach can generally be applied to any property and interpolates between the two end states. The following equation interpolates the relative permeability exponents:

$$K_r^t = (1 - w)\ K_r^A + w\, K_r^B, \tag{1}$$

where w is a mixing parameter that controls the shift of the saturation functions and is taken as a proxy for the chemical reactions that drive WA, expressed as follows:

$$w = \min\left(w_{max}, t_e/T\right), \tag{2}$$

where w_{max} is the maximum value of the mixing parameter $[0, 1]$, T is the time required to reach w_{max}, and t_e is the time of CO_2 exposure in the grid block above a threshold and is expressed as follows:

$$t_e = \int_0^t H\left(S_{CO_2}(\tau) - S_{\text{onset}}\right) d\tau, \tag{3}$$

where S_{onset} is the saturation threshold, after which the alteration begins. H(z) is the Heaviside step function, which allows the exposure time to be calculated only when the CO_2 saturation exceeds the onset threshold saturation. The Heaviside step function is defined as follows:

$$\mathrm{H}(\mathrm{z}) = 1 \text{if } \mathrm{z} > 0; \mathrm{H}(\mathrm{z}) = 0 \text{ if } \mathrm{z} \leq 0. \tag{4}$$

This modeling approach is an extension of the work conducted by Zhang et al. (2025), as it follows the same modeling structure but adds a maximum magnitude for the shifting parameter, w_{max}. This addition enhances flexibility in assessing a CCS case, as different rocks have different tendencies to undergo WA, and the application of a maximum cap accounts for this fact. Additionally, the study adopted S_{onset} as a physically uncertain parameter; in [13], it was a numerical threshold to prevent noise from being considered as a gas presence. However, in this study, we investigated whether the parameter would have a physical meaning, as being the required S_{CO_2} to establish contact with the rock surface to commence WA. This study assessed the sensitivity of dynamic WA by varying w_{max}, T, and S_{onset} separately and evaluating the effect on the saturation front extent.

2.2. Governing Equations and Numerical Simulation.

We start by considering the component balance [8]:

$$\frac{\partial}{\partial t}\left(S_\alpha \rho_\alpha \phi\right) + \nabla \cdot \left(\rho_\alpha \overrightarrow{v_\alpha}\right) - \rho_\alpha q_\alpha = 0, \quad \alpha \in \{\mathrm{CO_2}, \mathrm{w}\}, \tag{5}$$

subject to the constraint

$$S_\mathrm{w} + S_{CO_2} = 1, \quad 0 \leq S_\alpha \leq 1, \quad \alpha \in \{\mathrm{CO_2}, \mathrm{w}\}. \tag{6}$$

The phase flux is expressed by Darcy's law:

$$\vec{v} = -\frac{K}{\mathrm{m}}\left(\nabla p + \rho g \nabla z\right) \tag{7}$$

For relative permeabilities,

$$K_{r,g}^{\text{Drainage}} = \left(\frac{1 - S_w}{1 - S_{w,\text{irr}}}\right)^{N_g} \tag{8}$$

$$K_{r,w}^{\text{Drainage}} = \left(\frac{S_w - S_{w,\text{irr}}}{1 - S_{w,\text{irr}}}\right)^{N_w} \tag{9}$$

where S_w is the water saturation, $S_{w,irr}$ is the irreducible water saturation, N_g is the gas phase exponent, and N_w is the water phase exponent.

The governing equations were discretized using the finite volume method in which the spatial fluxes were approximated using the two-point flux approximation (TPFA). TPFA is a reasonable discretization approach because the grids are orthogonal, and the permeability is isotropic. An upwinding scheme was employed to evaluate the saturation-dependent properties at grid faces.

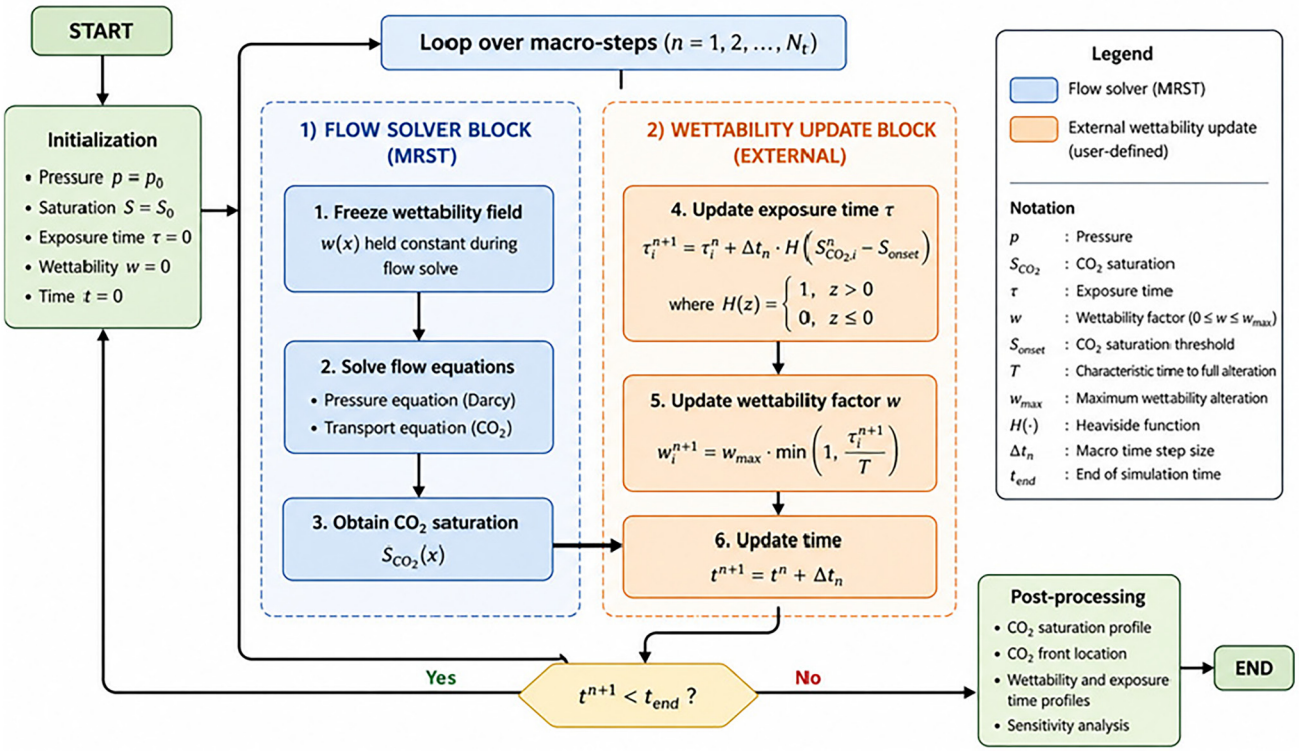

Figure 1. Sequential coupling algorithm for dynamic WA

Upwinding is a first-order accurate scheme that assumes that the values within a grid cell are uniform, considering the values of the upstream grid center.

The resulting nonlinear system was discretized in time using a fully implicit scheme, allowing for extended time steps and enhanced stability. The simulation was developed using the MATLAB Reservoir Simulation Toolbox (MRST) [8].

2.3. Sequential Coupling Implementation. The model and WA were implemented using a sequentially coupled approach in MRST in which the flow equations were solved using the reservoir simulator, and the WA model was updated externally. Coupling was controlled using a macroparameter that defined the frequency at which the system state was evaluated and the WA model was updated.

The approach consisted of an outer loop over macrosteps, in which WA-related parameters such as exposure time and wettability factor were initialized and tracked per grid cell. Within each macrostep, the solver advanced the simulation over several timesteps. When the macrostep was complete, the results were evaluated for the WA conditions. When $S_{CO_2} > S_{onset}$, the exposure time was updated by adding the total duration of the macrostep; otherwise, the simulation proceeded without modification.

Checking and logic handling were implemented using vectorized operations across all the grid cells. Following the update of the exposure time, the wettability factor was updated accordingly and used in the next macrostep.

2.4. Model Description. In this study, 1D immiscible drainage was analyzed, with CO_2 injected into an aquifer. 1D drainage conditions were selected to isolate the effect of WA from the impacts of the flow direction in multiple dimensions and gravity. The model descriptions are summarized in Table 2.

The curves used for relative permeability are presented in Table 3.

3. RESULTS AND DISCUSSION

3.1. Comparison of Static Curves. We began by running a full simulation for Cases A and B. The results are presented in Figure 2.

The saturation front of Case A travelled a larger distance than that of Case B. This may be because Case A was water-wet, providing more mobility to the CO_2 phase to travel further. In Case B, a banking effect of CO_2 was observed; the front was shorter and sharper than that in Case A. This finding is consistent with the results of previous wettability studies.

Table 2. *Simulation setup and parameters*

Group	Parameter	Value	Description
General Setup & Grid	Mesh Type	Cartesian	1D uniform grid setup
General Setup & Grid	Grid Dimensions (N_x N_y N_z)	1000 ×1 ×1	1000 cells in the x-direction
General Setup & Grid	Physical Size (L_x L_y L_z)	100 m ×1 m ×1 m	Total domain length is 100 m
General Setup & Grid	Simulation Time	730 days (2 years)	Total duration of the simulation
General Setup & Grid	Reporting Time Steps	2920 steps of 8 h	Fine resolution to ensure stability for the saturation functions alteration.
General Setup & Grid	Macrosteps	730 steps of 1 day	The checking and alteration of wettability are performed daily.
Petrophysics	Absolute Permeability (K)	0.1 Darcy	Uniform across the entire domain.
Petrophysics	Porosity (phi)	0.20 (20%)	Uniform across the entire domain
Fluid Properties	Fluid Phases	Water and CO_2	Two-phase immiscible flow
Fluid Properties	Water Reference Density (rho_L)	1000 kg/m^3	Represents water or heavy oil
Fluid Properties	CO_2 Reference Density (rho_V)	700 kg/m^3	Represents dense injected gas / CO_2
Fluid Properties	Water Viscosity (mu_L)	1e-3 Pa*s (1 cP)	Viscosity of the wetting phase
Fluid Properties	CO_2 Viscosity (mu_V)	0.05e-3 Pa*s (0.05 cP)	Viscosity of the non-wetting phase
Initial Conditions	Initial Reservoir Pressure (P0)	150 bar	Uniform starting pressure
Initial Conditions	Initial Saturation (SL SV)	$S_w = 1.0$; $S_{CO_2} = 0.0$	Reservoir initially 100% saturated with water
Boundary Conditions & Wells	Injector Position	Cell (1,1,1)	Located at x = 0 m (inlet), used to simulate a Neumann boundary condition
Boundary Conditions & Wells	Injector Control	Constant Total Volume Rate	Targets exactly 5% of total reservoir pore volume over 365 days, a Neumann-type boundary condition
Boundary Conditions & Wells	Injector Fluid Composition	100% CO_2	Injecting pure gas phase
Boundary Conditions & Wells	Producer Position	Cell (1000,1,1)	Located at x = 100 m (outlet)
Boundary Conditions & Wells	Producer Control	Constant Bottom Hole Pressure	Maintains BHP at 150 bar, simulating an infinite aquifer away from the simulation case (Dirichlet condition)

Table 3. *Relative permeability curves for Cases A and B*

Group	Parameter	Value	Description
Relative Permeability	Case A	$N_w = 7.0; N_g = 1.5$	Highly mobile gas, restricted liquid flow
Relative Permeability	Case B	$N_w = 3.5; N_g = 3.0$	Gas less mobile, liquid slightly more mobile

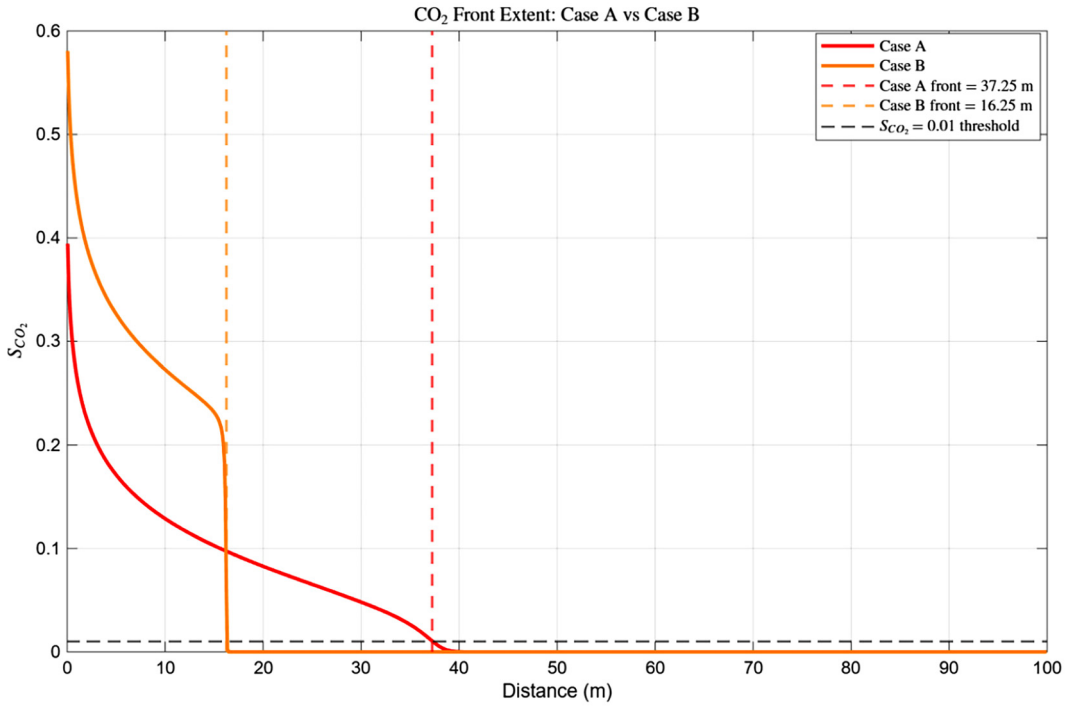

Figure 2. CO_2 front extent comparison between Cases A and B

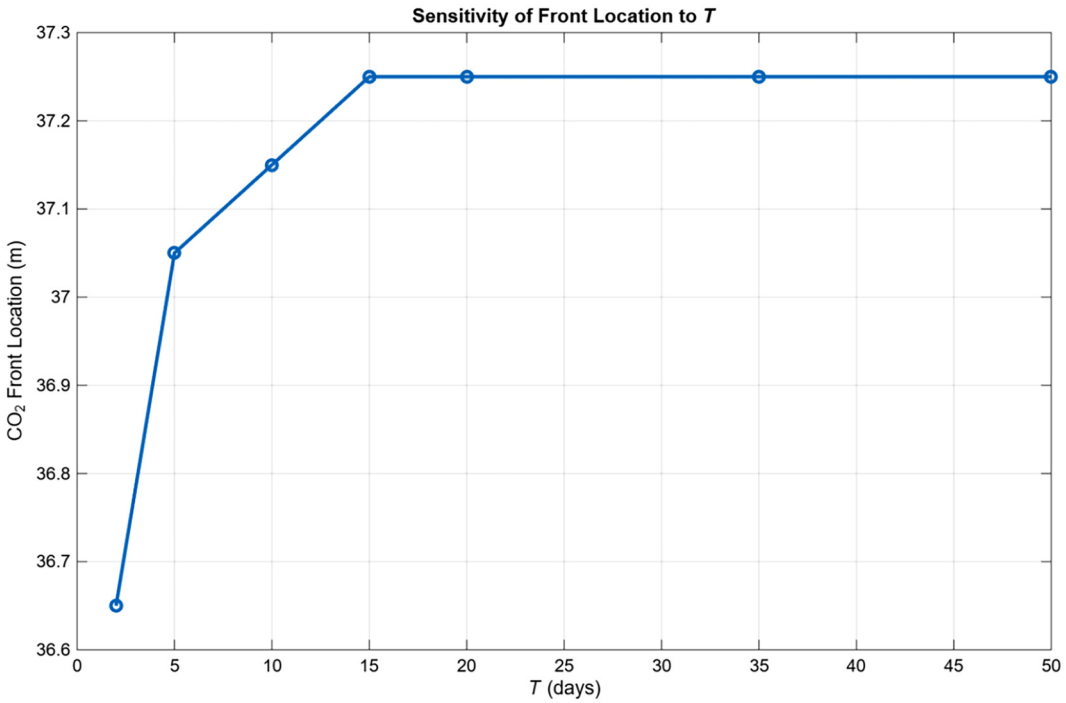

Figure 3. Sensitivity of CO_2 front location to characteristic time T

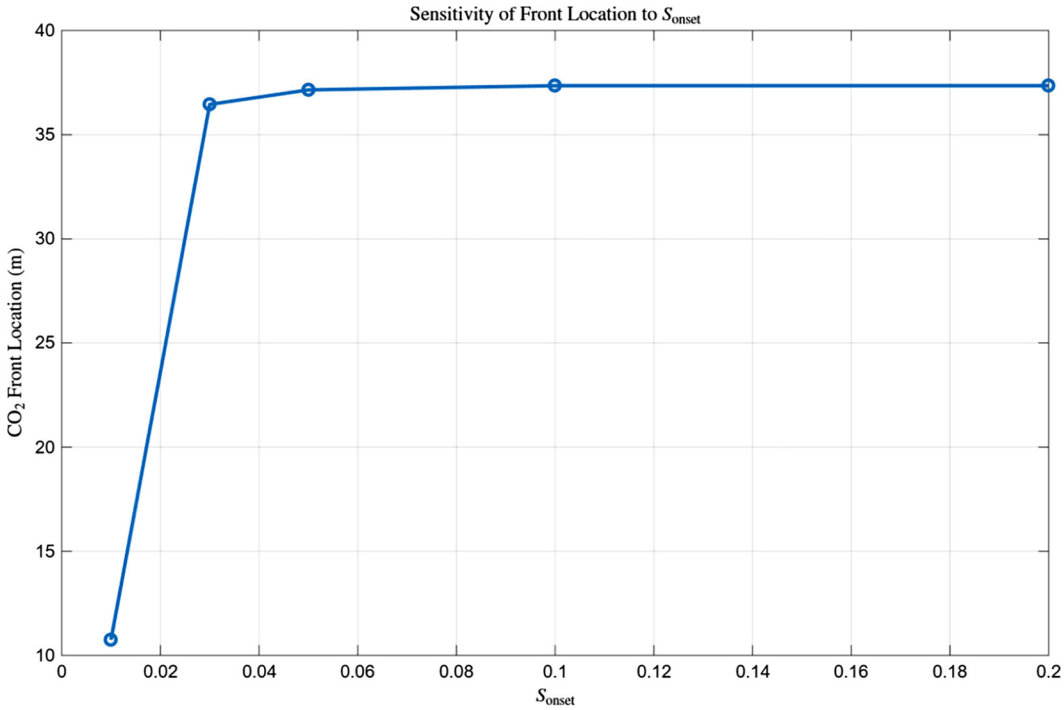

Figure 4. Sensitivity of CO_2 front location to onset saturation S_{onset}

This trend also holds when considering dynamic effects, that is, a shift from Case A to Case B. Therefore, we sought to investigate the effects of various parameters used in the WA model.

3.2. Effect of Characteristic Time T. We began the analysis by considering variations in T. As highlighted in Subsection 3.1, T governs the time to reach w_{max} and can be considered a property of the reactivity of the rock. We adopted $w_{max} = 1$ and $S_{onset} = 0.05$. The range was selected from 0 to 50 days to evaluate the short-term effects and aligned with the literature on aging duration.

As T increased, the system exhibited a slower alteration from Case A to Case B and remained in Case A longer; therefore, the effects are more dominated by Case A. The front travelled longer as T increased. By contrast, a lower T value indicates a faster alteration to Case B, and the system behaves closer to Case B. This was demonstrated by a shorter front development.

3.3. Effect of Onset Saturation S_{onset}. The effect of S_{onset} was analyzed. In this analysis, T = 10 and $w_{max} = 1$. A lower S_{onset} value indicates that the system changes faster, even at lower saturations. However, a high S_{onset} shows that the system requires time for saturation in the grid to reach the level. The range was selected from 0.01, indicating that the system required minimal exposure to initiate WA. A high value (0.2) was selected to understand the sensitivity behavior of the model with respect to the parameter. We observed a similar trend and behavior with respect to T.

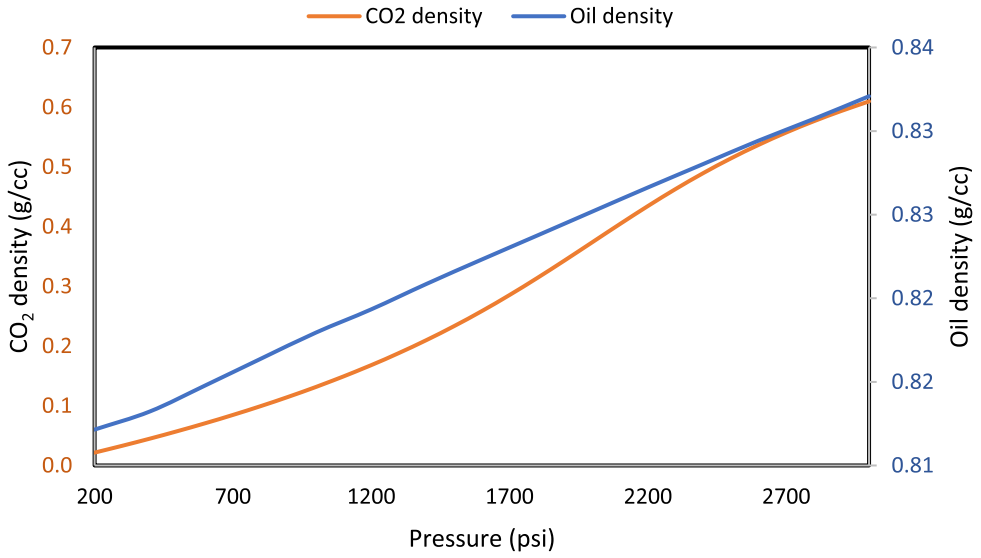

Figure 5. Sensitivity of CO_2 front location to w_{max}

This high sensitivity at the early stage shows that the Heaviside activation function was utilized, and the behavior of the system converged to that of Case A, even when slightly higher S_{onset} values were used. S_{onset} significantly influenced the system, as it determined which parts of the CO_2 front underwent WA. Typically, this would affect the overall behavior of the system under the examined conditions.

3.4. Effect of Maximum WA w_{max}. Finally, w_{max} was considered, where T = 10 and S_{onset} = 0.05. This range reflects the behavior of w_{max} as a cap on the alteration. 0.2 was the initial value at which alteration was allowed to proceed but was capped close to Case A; 1 is a complete alteration toward Case B.

The conditions show that at low w_{max}, the system behavior was the same as that in Case A; it behaved as a strongly water-wet system. This occurred only when w_{max} was allowed to attain higher values, and changes were observed in the front location. In this case, the change was insignificant, with only 0.1 m, which is the same as the grid resolution adopted in the study. This could indicate that either the resolution limit or the model response to the parameter alone is not significant.

The results were consistent across all the parameters. The plume was delayed as the WA proceeded and became higher or faster. These results are consistent with the results of a 1D study by[7].

4. CONCLUSIONS

This study investigated the effects of dynamic WA during constant-rate CO_2 injection into saline aquifers and through numerical experiments, determined the potential deviations caused by time-dependent alteration in the CO_2 saturation front extent. At the field scale, the reduced CO_2 front migration associated with dynamic wettability alteration may limit plume extent and potentially enhance storage security; however, closed-system assessments are needed to evaluate potential pressure buildup risks. In the current model, S_{onset} controlled most of the sensitivity, as it controlled the parts of the front that underwent change, followed by T, which reflected the speed at which alteration occurred. Finally, w_{max} had the least effect on front evolution under the analyzed conditions.

The sensitivity analysis conducted was one-at-a-time sensitivity, and interactions between parameters and global sensitivity analysis should be conducted to clarify the model behavior and sensitivity. The simulation setup was highly idealized and simplified. This was performed to isolate WA from other effects that could shape the response. For field-scale-effect investigations, the use of a heterogeneous anisotropic geological model would show the behavior in the aquifer more accurately. The simplified WA model and simulation case showed that the saturation front was sensitive to wettability dynamics. However, the extent of this alteration and the magnitude of the effect require more thorough investigations using more realistic reservoir and aquifer models. The upwinding discretization scheme is limited because it does not capture the fronts satisfactorily. Future studies should consider using accurate higher-order numerical schemes.

Although the model is simple to design, it has key limitations. First, the alteration accumulated above the saturation threshold irrespective of the saturation of the grid cell. That is, a cell just above the threshold and a cell significantly above it accumulate exposure time at an equal rate. Another challenge is that the model is not smooth. The utilization of the Heaviside function, although conceptually clean, introduces edges and no differentiability. This is a challenge for the numerical stability of solvers and requires finer time steps when running the model, which increases the runtime. Moreover, this study used an immiscible model and saturation as drivers of alteration. This is a proxy. Realistically, the dissolved CO_2 in brine would cause the highest effect. Therefore, utilizing a compositional model that enables mass transfer between phases is more representative.

Hard Heaviside-onset activation is a well-known limitation. Very low S_{onset} values can induce WA to accumulate in the low-saturation CO_2 plume tail, causing large sensitivity and switch-like behavior. This should be treated as a modeling limitation, rather than a code bug. Additionally, WA influences the capillary pressure, which in turn plays a role in the saturation front evolution.

AFFILIATIONS AND AUTHOR DETAILS

Undergraduate Author

Khaled Muteb Alrashidi – *Department of Petroleum Engineering, King Fahd University of Petroleum & Minerals, Dhahran 31261, Saudi Arabia;* 0009-0000-1697-2304
Email: s202222180@kfupm.edu.sa

Corresponding Author

Arshad Raza – *Research Mentor, Assistant Professor, Department of Petroleum Engineering, King Fahd University of Petroleum & Minerals, Dhahran 31261, Saudi Arabia;* 0000-0001-7706-1002
Email: arshad.raza@kfupm.edu.sa

ACKNOWLEDGEMENTS

We thank King Fahad University of Petroleum and Minerals (KFUPM) for supporting this research project.

REFERENCES

(1) Alalaiwat, D., & Khan, E. (2023). Current status and future scenarios of carbon capture from power plants emission: A review. *Reviews in Environmental Science and Bio/Technology*, *22*, 1–24. https://doi.org/10.1007/s11157-023-09663-2

(2) Al-Khdheeawi, E. A., Vialle, S., Barifcani, A., Sarmadivaleh, M., & Iglauer, S. (2017). Impact of reservoir wettability and heterogeneity on CO_2-plume migration and trapping capacity. *International Journal of Greenhouse Gas Control*, *58*, 142–158. https://doi.org/10.1016/j.ijggc.2017.01.012

(3) Alsalman, M., Raza, A., Mahmoud, M., Murtaza, M., Arif, M., Isah, A., Alafnan, S., & Shahzad Kamal, M. (2024). Experimental Assessment of Time Dependent Wettability Alteration in CO_2-Brine-Rock System. *SPE Conference at Oman Petroleum & Energy Show*, D011S002R005. https://doi.org/10.2118/218815-MS

(4) Blunt, M. J. (2017). *The Imperial College Lectures in Petroleum Engineering: Volume 2: Reservoir engineering*. World Scientific.

(5) Chai, R., Ma, Q., Goodarzi, S., Yow, F. Y., Bijeljic, B., & Blunt, M. J. (2025). Multiphase Reactive Flow During CO_2 Storage in Sandstone. *Engineering*, *48*, 81–91. https://doi.org/10.1016/j.eng.2025.01.016

(6) Gholami, R., & Raza, A. (2022). CO_2 sequestration in sandstone reservoirs: How does reactive flow alter trapping mechanisms? *Fuel*, *324*, 124781. https://doi.org/10.1016/j.fuel.2022.124781

(7) Kassa, A. M., Gasda, S. E., Landa-Marbán, D., Sandve, T. H., & Kumar, K. (2022). Field-scale impacts of long-term wettability alteration in geological CO2 CO_2 storage. *International Journal of Greenhouse Gas Control*, *114*, 103556. https://doi.org/10.1016/j.ijggc.2021.103556

(8) Lie, K.-A., & Møyner, O. (Eds.). (2021). *Advanced Modeling with the MATLAB Reservoir Simulation Toolbox* (1st ed.). Cambridge University Press. https://doi.org/10.1017/9781009019781

(9) Luo, A., Li, Y., Chen, X., Zhu, Z., & Peng, Y. (2022). Review of CO_2 sequestration mechanism in saline aquifers. *Natural Gas Industry B*, *9*(4), 383–393. https://doi.org/10.1016/j.ngib.2022.07.002

(10) Metz, B. & Intergovernmental Panel on Climate Change (Eds.). (2005). *IPCC special report on carbon dioxide capture and storage*. Cambridge University Press, for the Intergovernmental Panel on Climate Change.

(11) Paltsev, S., Morris, J., Kheshgi, H., & Herzog, H. (2021). Hard-to-Abate Sectors: The role of industrial carbon capture and storage (CCS) in emission mitigation. *Applied Energy*, *300*, 117322. https://doi.org/10.1016/j.apenergy.2021.117322

(12) Zhang, H., Al Kobaisi, M., & Arif, M. (2023). Impact of wettability and injection rate on CO_2 plume migration and trapping capacity: A numerical investigation. *Fuel*, *331*, 125721. https://doi.org/10.1016/j.fuel.2022.125721

(13) Zhang, H., Al Kobaisi, M., & Arif, M. (2025). Field-scale investigations on long-term dynamic wettability alteration in underground CO_2 storage. *Energy*, *333*, 137261. https://doi.org/10.1016/j.energy.2025.137261